

Tunable ultraviolet radiation by second-harmonic generation in periodically poled lithium tantalate

J.-P. Meyn* and M. M. Fejer

E. L. Ginzton Laboratory, Stanford University, Stanford, California 94305

Received April 14, 1997

We describe electric-field poling of fine-pitch ferroelectric domain gratings in lithium tantalate and characterization of nonlinear-optical properties by single-pass quasi-phase-matched second-harmonic generation (QPM SHG). With a $7.5\text{-}\mu\text{m}$ -period grating, the observed effective nonlinear coefficient for first-order QPM SHG of 532-nm radiation is 9 pm/V , whereas for a grating with a $2.625\text{-}\mu\text{m}$ period, 2.6 pm/V was observed for second-order QPM SHG of 325-nm radiation. These values are 100% and 55% of the theoretically expected values, respectively. We derive a temperature-dependent Sellmeier equation for lithium tantalate that is valid deeper into the UV than currently available results, based on temperature-tuning experiments at different QPM grating periods combined with refractive-index data in the literature. © 1997 Optical Society of America

Single-pass frequency conversion of near-infrared lasers is an attractive approach for the generation of blue and UV coherent radiation. Noncritical phase matching and a high effective nonlinear coefficient d_{eff} are necessary for high conversion efficiency in such applications. Quasi-phase matching^{1,2} (QPM) always permits noncritical phase matching and the use of the large diagonal nonlinear coefficients d_{33} , which are inaccessible with birefringent phase matching. Periodically poled ferroelectrics have been widely exploited for QPM interactions, although applications in the visible and the UV have been challenging because of difficulties in the fabrication of the fine-pitch domain gratings necessitated by the short coherence lengths involved. Lithium tantalate (LiTaO_3) is transparent to 280 nm and is therefore more suitable for nonlinear-optical interactions in the mid UV than lithium niobate (LiNbO_3), which is transparent to 330 nm.

Second-harmonic generation (SHG) in the UV to wavelengths as short as 340 nm and domain gratings to periods as short as $1.7\text{ }\mu\text{m}$ have been reported.³ In this Letter we report SHG down to 325 nm, measurement of the effective nonlinear coefficient, temperature tuning over 7 nm at the second harmonic, and a temperature-dependent Sellmeier equation that is valid into the UV.

The poling process applied here to LiTaO_3 was similar to that described for lithium niobate.⁴ Our starting material was commercial 2-in.- (51-mm-) diameter z -cut crystal wafers⁵ with thicknesses of 200, 300, or $500\text{ }\mu\text{m}$ in different experiments. Periodic aluminum electrodes were patterned on the $c+$ face of the LiTaO_3 crystal wafers by a lithographic lift-off process, with the grating \mathbf{k} vectors parallel to the crystal y axis. The $c+$ electrode was covered with electrically insulating photoresist (Shipley 1400-33), except for an outer 1-mm-wide ring. This contact region of the $c+$ face and the entire $c-$ face were connected to a high-voltage circuit by a sodium chloride solution acting as a liquid contact. Circular patterns from 3- to 16-mm diameter were poled. The duty cycle was controlled by the amount of charge delivered to the sample. For 50% duty cycle this is the spontaneous polarization, $P_s = 0.65\text{ C/m}^2$. We achieved uniform domain nucle-

ation by using $0.5\text{--}1.0\text{-}\mu\text{m}$ thin electrodes and permitting the domains to spread under the insulator. After poling, we etched the crystals in hydrofluoric acid at room temperature for 20 min to reveal the domains. The domain patterns on the $c+$ and the $c-$ faces of a $200\text{-}\mu\text{m}$ -thick crystal with a $2.625\text{-}\mu\text{m}$ period are shown in Fig. 1. The diameter of the poled region is 3 mm, for which a poling current of 1 mA was applied for 6.5 ms. The duty cycle shows some variation, but it is close to 75%, which is the optimum duty cycle for second-order QPM.

Phase-matching wavelength and efficiency were measured for a number of crystals by single-pass SHG with a TEM_{00} -mode pump beam obtained from a Ti:sapphire laser (700–930 nm), a cw dye laser (640–660 nm), or a Nd:YAG laser (1064 nm). The Ti:sapphire and the dye lasers were operated with a birefringent filter and an etalon; wavelengths were measured with a fiber-coupled wavemeter. In all cases nearly confocal focusing was used.

All the periodically poled LiTaO_3 crystals were heated in an oven for tuning to the phase-matching wavelength. The oven temperature was monitored with a platinum resistive temperature device (RTD) element and controlled to within $0.1\text{ }^\circ\text{C}$. No photorefractive damage was observed at temperatures above $170\text{ }^\circ\text{C}$. At lower temperatures we observed beam distortion.

For quantitative efficiency measurements, the input and output powers were measured with a calibrated powermeter (Newport Model 835). The fundamental radiation was blocked with Schott filter UG 11 or BG 39, depending on the spectral range; we confirmed com-

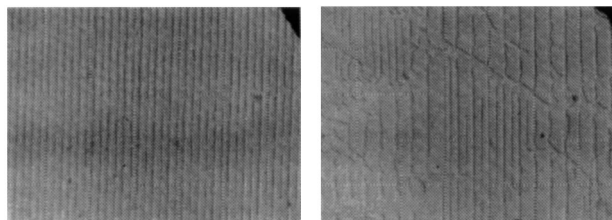


Fig. 1. $c+$ face (left) and $c-$ face (right) of periodically poled LiTaO_3 , with a grating period $\Lambda = 2.625\text{ }\mu\text{m}$.

plete blocking by tuning the laser out of the phase-matching peak and measuring the residual transmitted power. For wavelength-tuning data, we estimated the peak visually by monitoring the UV output on a fluorescent card.

All efficiency calculations were performed under the assumption of diffraction-limited beam propagation and confocal focusing. Since the crystals were uncoated and wedged, we took into account the Fresnel reflections at the surfaces to calculate the internal conversion efficiency. For single-longitudinal-mode pump radiation, the effective nonlinear coefficient is calculated from⁶

$$d_{\text{eff}} = \left[\frac{P_{\text{out}}}{(P_{\text{in}})^2} \frac{\lambda_{\omega}^3 n_{\omega} n_{2\omega} \epsilon_0 c}{16\pi^2 l} \frac{1}{h} \right]^{1/2}, \quad (1)$$

where P_{in} is the fundamental power inside the crystal, P_{out} is the corresponding second-harmonic power, λ_{ω} is the fundamental wavelength, n is the refractive index evaluated at the frequency given in the subscript, l is the crystal length, ϵ_0 is the dielectric constant, and c is the speed of light. The factor h is a dimensionless coefficient that quantifies the effect of focusing and birefringence and is of the order of unity near optimal focusing for noncritically phase-matched interactions.⁷ The effective nonlinear coefficient for an ideally modulated QPM crystal is $d_{\text{eff}} = (2/\pi m)d_{33}$, with m being the QPM order. Duty-cycle variations and other defects can reduce the effective nonlinear coefficient.² The results of the efficiency measurements on representative crystals are summarized in Table 1.

A recent measurement⁸ for d_{33} of LiTaO₃ is 13.8 pm/V at 1064 nm and 15.1 pm/V at 852 nm. Therefore the crystals used for SHG at 532 and 483 nm with $d_{\text{eff}} = 9$ pm/V have theoretical efficiency within experimental error. We also measured the temperature-tuning bandwidth for SHG of 1064 nm in the 16-mm-long crystal. The FWHM of 1.6 K is again within the experimental uncertainty of the theoretical bandwidth calculated with the temperature-dependent Sellmeier relation given below, indicating that the grating and the refractive index of the substrate are adequately uniform for interactions at least to this length.

The nonlinearity of the crystals used in second-order QPM is a factor of 2 less than the theoretical value of 4.7 pm/V. The crystal with $\Lambda = 5.5 \mu\text{m}$ had a duty cycle of $\sim 60\%$, which is more suitable for first-order QPM. For second-order QPM, a 60% duty cycle leads to an expected reduction of 0.59 in d_{eff} from that obtained for the ideal 75% duty cycle.²

For the crystal with $\Lambda = 2.625 \mu\text{m}$ both the absorption at the second-harmonic and the duty-cycle variations are sources for decreased conversion ef-

iciency. The absorption at the second harmonic at 325 nm was estimated by absorption measurement in a thin wafer to be 1.7 cm^{-1} . According to the model,⁹ the output power is decreased by 23% by absorption for this particular sample. With this decrease taken into account, the effective nonlinear coefficient is $d_{\text{eff}} = 2.6 \text{ pm/V}$. The calculation after Eq. (1) using the numbers given in Table 1 yields 2.3 pm/V. The remaining difference from the theoretical value of 4.7 pm/V can be explained with duty-cycle variations of the order of $0.3 \mu\text{m}$.²

In all cases the highest efficiency was found near the $c+$ face of the crystal, where the domain uniformity was best. For various positions along the x direction in the crystal, the efficiency varied by a factor of 2; the values given above are repeatable over approximately half the aperture of the crystal.

Accurate refractive-index data are necessary for designing QPM devices with phase matching at a desired temperature, especially in the UV, where both the refractive index and the thermo-optic coefficient vary rapidly with wavelength. Results were given for a temperature-dependent Sellmeier relation for LiTaO₃,¹⁰ but this relation, developed with data taken only over the range 450–4000 nm, is inadequate for predicting our observed phase-matching data, especially at the shorter UV wavelengths.

The most straightforward method of obtaining dispersion data is to fit a Sellmeier relation to refractive indices measured at a number of wavelengths and temperatures, taking care that the wavelength range of the data exceeds that over which an accurate representation is required, since extrapolation of Sellmeier relations is unreliable. As we were not equipped for such temperature-dependent refractive-index measurements in the UV, we adopted a somewhat less direct approach, using a data set consisting of literature values for the room-temperature refractive indices for 21 wavelengths over the range $0.45\text{--}4.0 \mu\text{m}$,¹¹ along with the wavelengths for QPM SHG in the UV for 245 combinations of grating period and temperature. The latter data are shown in Fig. 2.

The QPM period for phase-matching SHG is related to the refractive indices at the fundamental and the second-harmonic wavelengths by

$$\Lambda = \frac{\lambda_{\omega}}{2(n_{2\omega} - n_{\omega})}. \quad (2)$$

We took into account the crystal thermal expansion by modifying the grating period according to the thermal-expansion coefficient given in Ref. 12:

$$\Lambda(T) = \Lambda(20^\circ\text{C})[1.6 \times 10^{-5}(T - 20^\circ\text{C}) + 7 \times 10^{-9}(T - 20^\circ\text{C})^2]. \quad (3)$$

Table 1. Efficiency and Nonlinear Coefficients of Selected Periodically Poled LiTaO₃ Crystals

Λ (μm)	m	Thickness (mm)	Length (mm)	λ_{SHG} (nm)	P_{in} (mW)	P_{out} (μW)	d_{eff} (pm/V)
7.5	1	0.5	16	532	191	490	9
5.5	1	0.3	16	483	64	75	9
5.5	2	0.3	16	394	384	303	2.3
2.625	2	0.2	3	325	133	11.5	2.6

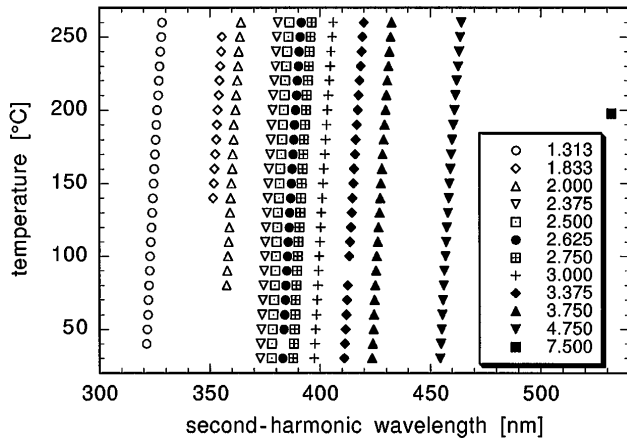


Fig. 2. Phase-matching temperatures for QPM SHG as a function of second-harmonic wavelength for 12 different periods, shown in micrometers in the legend. Higher-order QPM periods are quoted as equivalent first-order periods for clarity of presentation.

Initially, we attempted to represent the refractive-index data in a form similar to that previously applied to both LiNbO_3 and LiTaO_3 (Refs. 10, 13, and 14):

$$n_e^2(\lambda, T) = [A + a(T)] + \frac{B + b(T)}{\lambda^2 - [C + c(T)]^2} + D\lambda^2. \quad (4)$$

We adjusted the parameters in Eq. (4) by minimizing the quadratic errors, using a Levenberg–Marquard algorithm implemented in a commercial software package.¹⁵ The resulting expression predicted both the phase-matching data and the refractive-index data¹¹ of the data set with reasonable accuracy, but systematic residuals remained, especially at the deeper UV wavelengths. We thus added a second pole to the Sellmeier relation,

$$n_e^2(\lambda, T) = A + \frac{B + b(T)}{\lambda^2 - [C + c(T)]^2} + \frac{E}{\lambda^2 - F^2} + D\lambda^2, \quad (5)$$

and repeated the fitting procedure. We found that the sum of the quadratic errors was reduced by more than a factor of 2 with the additional pole. No statistically significant improvement in the fit was obtained when the second pole was permitted to be temperature dependent. The parameters of the fit are as follows:

$$\begin{aligned} A &= 4.5284, \\ B &= 7.2449 \times 10^{-3}, \\ C &= 0.2453, \\ D &= -2.3670 \times 10^{-2}, \\ E &= 7.7690 \times 10^{-2}, \\ F &= 0.1838, \\ b(T) &= 2.6794 \times 10^{-8} (T + 273.15)^2, \\ c(T) &= 1.6234 \times 10^{-8} (T + 273.15)^2. \end{aligned}$$

With this fit, all the phase-matching data are predicted with an accuracy of better than $0.005 \mu\text{m}$ in QPM period or 2.5 K in phase-matching temperature. We observed a systematic sample-to-sample variation in the residuals in addition to random error of the

order of $0.002 \mu\text{m}$ in the QPM period. Typically the crystals from one batch of wafers had negative residuals, whereas crystals from a second batch had positive residuals. Since we used different vendors, differences in the crystal-growth procedure, e.g., composition, are likely to change the dispersion only slightly.

In conclusion, we have demonstrated that periodically poled LiTaO_3 can be fabricated for noncritically phase-matched SHG deeper into the UV than is possible in LiNbO_3 or KTiOPO_4 , with an effective nonlinear coefficient that is competitive with the best available birefringent materials. We have developed a temperature-dependent Sellmeier relation that accurately predicts QPM wavelengths over the tested range 532–325 nm and 20–260 °C. We plan to focus on optimizing the crystal quality, especially for periods of less than $3 \mu\text{m}$ for first-order UV generation, and on refining the temperature-dependent Sellmeier relation by inclusion of infrared data from optical parametric oscillator tuning behavior. Further research on crystal growth and postgrowth processing is required for improved transparency in the mid UV range.

We thank the Advanced Research Projects Agency for support through the Center for Nonlinear Optical Materials and the Optoelectronic Materials Center, and Shin-Etsu, Japan, for donation of LiTaO_3 wafers. J.-P. Meyn acknowledges financial aid from Deutsche Forschungsgemeinschaft within contract Me 1429/2-1.

*Present address, Universität Kaiserslautern, Fachbereich Physik, Erwin-Schrödinger-Strasse 46, 67663 Kaiserslautern, Germany.

References

1. J. A. Armstrong, N. Bloembergen, J. Duncan, and P. S. Pershan, *Phys. Rev.* **127**, 1918 (1962).
2. M. M. Fejer, G. A. Magel, D. H. Jundt, and R. L. Byer, *IEEE J. Quantum Electron.* **28**, 2631 (1992).
3. K. Mizuuchi, K. Yamamoto, and M. Kato, *Appl. Phys. Lett.* **70**, 1201 (1997).
4. L. E. Myers, R. C. Eckhard, M. M. Fejer, and R. L. Byer, *J. Opt. Soc. Am. B* **12**, 2102 (1995).
5. LiTaO_3 wafers were manufactured by Shin-Etsu Kagaku Kougyou, 2-6-1 Ohtemachi Chiyodaku 100, Japan, and Yamaju Ceramics, 971 Anada-cho Setoshi, 489 Japan.
6. G. D. Boyd and D. A. Kleinman, *J. Appl. Phys.* **39**, 3597 (1968).
7. V. Pruneri, S. D. Butterworth, and D. C. Hanna, *Opt. Lett.* **21**, 390 (1996).
8. I. Shoji, T. Kondo, A. Kitamoto, M. Shirane, and R. Ito, "Absolute scale of the second-order nonlinear optical coefficients," *J. Opt. Soc. Am. B* (to be published).
9. M. L. Bortz, S. J. Fields, M. M. Fejer, D. W. Nam, R. G. Waarts, and D. F. Welch, *IEEE J. Quantum Electron.* **30**, 2953 (1994).
10. K. S. Abedin and H. Ito, *J. Appl. Phys.* **80**, 6561 (1996).
11. W. L. Bond, *J. Appl. Phys.* **36**, 1674 (1965).
12. Y. S. Kim and R. T. Smith, *J. Appl. Phys.* **40**, 4637 (1969).
13. S. Matsumoto, *Electron. Lett.* **27**, 2040 (1991).
14. G. J. Edwards and M. Lawrence, *Opt. Quantum Electron.* **16**, 373 (1984).
15. Pro-fit 5.0 (Quantum-Soft, Zürich, Switzerland, 1996).